Published in final edited form as:
J Phys Chem B. 2010 March 25; 114(11): 4070–4081. doi:10.1021/jp1006704.

Adsorption of α-Synuclein on Lipid Bilayers: Modulating the Structure and Stability of Protein Assemblies

Farzin Haque[†], **Anjan P. Pandey**[†], **Lee R. Cambrea**[†], **Jean-Christophe Rochet**[‡,*], and **Jennifer S. Hovis**[†,*]

[†]Department of Chemistry, Purdue University, West Lafayette, IN 47907.

[‡]Department of Medicinal Chemistry and Molecular Pharmacology, Purdue University, West Lafayette, IN 47907.

Abstract

The interaction of α-synuclein with phospholipid membranes has been examined using supported lipid bilayers and epi-fluorescence microscopy. The membranes contained phosphatidylcholine (PC) and phosphatidic acid (PA), which mix at physiological pH. Upon protein adsorption the lipids undergo fluid-fluid phase separation into PC-rich and PA-rich regions. The protein preferentially adsorbs to the PA-rich regions. The adsorption and subsequent aggregation of α-synuclein was probed by tuning several parameters: the charge on the lipids, the charge on the protein, and the screening environment. Conditions which promoted the greatest extent of adsorption resulted in structurally heterogeneous aggregates, while comparatively homogeneous aggregates were observed under conditions whereby adsorption did not occur as readily. Our observation that different alterations to the system lead to different degrees of aggregation and different aggregate structures poses a challenge for drug discovery. Namely, therapies aimed at neutralizing α-synuclein must target a broad range of potentially toxic, membrane-bound assemblies.

Introduction

Recently there has been considerable interest in protein aggregation diseases, the hallmark of which is the fibrillization of one or more proteins.[1,2] The nature of the toxic species is in general unknown, and toxicity may be conferred through multiple pathways. In Parkinson's disease toxicity involves the aggregation of α-synuclein, a 14 kDa, presynaptic protein.[3–5] A number of functions have been ascribed to α-synuclein, including regulation of synaptic vesicle pools[6,7] and dopamine reuptake.[8]

In solution α-synuclein lacks a stable secondary structure.9 It avidly binds to anionic membranes by adopting a structure in which the first ~94 residues (of 140) form an α-helix that sits on top of the bilayer.10 The α-helix-forming region spans seven degenerate, 11-residue repeats, six of which contain a highly conserved motif 'KTK(E/Q)GV'. The face that interacts with the membrane is hydrophobic and is flanked by lysine residues at the nonpolar/polar interface.11–15 The NAC (non-Aβ component of Alzheimer's disease

*Corresponding Authors: (J-CR) rochet@pharmacy.purdue.edu, phone: (765) 494-1413, Fax (765) 494-6790; (JSH) jennifer.hovis@gmail.com, phone (419) 233-2378.

Supporting Information Available.
Fluorescence recovery after photobleaching of phase separated PA/PC bilayers; addition of different concentration of α-synuclein (0.26, 2.6 and 5.4 μM) at pH 5.0 and 7.4; quantification of α-synuclein adsorption and desorption on PC bilayers.

amyloid) domain (residues 61–95) is particularly hydrophobic and thought to be critically involved in the aggregation of α-synuclein.[11,16,17]

There are a wide variety of α-synuclein aggregates which can be formed in the solution phase (see 18 for a review): Fibrils, which have a diameter of 10 nm and a highly ordered β-sheet structure, are found in the proteinacous Lewy body deposits in Parkinson's brains.[19–22] Protofibrils, including spheres (2–5 nm in diameter), chains, and rings with extensive β-structure, are prefibrillar intermediates on the α-synuclein self-assembly pathway and have been shown to permeabilize membranes.[23–26] Unstructured/semi-structured aggregates that sample a variety of conformations, similar to small, conformationally flexible oligomers composed of the amyloid-β peptide, may also be formed by α-synuclein.[18]

There are conflicting reports in the literature regarding the role that membranes play in the aggregation of α-synuclein: evidence for both enhancement[27–30] and suppression[31,32] of aggregation has been reported. These disparate observations may be due to differences in experimental parameters, including protein-lipid ratios and phospholipid compositions.[33,34] The structures of membrane-bound α-synuclein aggregates have not been extensively characterized. β-Sheet-rich species similar to protofibrils or fibrils formed in solution may be present,[20,26,35–38] and α-helical oligomers may also be generated.[39] α-Synuclein has been shown to form helical oligomers in solutions containing fluorinated alcohols, a mimic for the membrane interface (Rochet unpublished data).[40] Recent work from our group identified three parameters that can be adjusted to tune α-synuclein aggregation: anionic lipid concentration, protein concentration and divalent ion concentration.[39] When the protein aggregates, a lateral reorganization of the mixed anionic/zwitterionic lipid bilayer is observed, resulting in the formation of anionic lipid-rich regions (corresponding to regions of clustered protein) and zwitterionic lipid-rich regions.

A central problem in the PD field is to identify conditions that promote the formation of toxic α-synuclein aggregates. α-Synuclein aggregation may result in toxicity through a variety of mechanisms, including (i) a loss of the protein's normal function;[6–8] (ii) interference with protein clearance mechanisms, including autophagy[41] and the ubiquitin-proteasome system[42–44]; and (iii) membrane permeabilization triggered by α-synuclein protofibrils.[26] To identify conditions under which α-synuclein becomes toxic it is necessary to consider that toxicity may be imparted by generic aggregation or by the formation of specific aggregated structures.

In this work we characterized the aggregation of α-synuclein on membranes enriched with the anionic lipid phosphatidic acid (PA). PA was chosen because it has been suggested that α-synuclein regulates synaptic vesicle formation and vesicle pool size by inhibiting phospholipase D (PLD), an enzyme that generates PA and whose activity is regulated by PA.[45–47] In addition, the charge on PA is tunable in a physiological range: pK_{a1} ~3.2 and pK_{a2} ~7.9.[48] By performing experiments at two different pH values, 5.0 and 7.4, we could examine the effect of changing the membrane charge density on membrane–protein interactions. The PA lipid was DOPA (1,2-dioleoyl-*sn*-glycero-3-phosphate) and the zwitterionic lipid was DOPC (1,2-dioleoyl-*sn*-glycero-3-phosphocholine). These lipids were chosen because they remain fluid at room temperature, and they have been the subject of exceedingly careful pK_a studies.[48] Membranes composed of 30 mol% DOPA/70 mol% DOPC were used in this study because our group has extensive experience with the physio-chemical properties of this lipid mixture.[49–51] Supported bilayers were chosen because they provide a convenient platform for both imaging (i.e. via epi-fluorescence microscopy) and exchanging solution conditions. Unlike giant unilamellar vesicles, which have very small Laplace pressures, supported bilayers can tolerate large changes in solution conditions without damage.

This study revealed that α-synuclein readily binds to membranes composed of PA and phosphatidylcholine (PC). Conditions that promote protein-protein contacts and lead to stable membrane-bound protein aggregates were elucidated. These findings have important implications on our understanding of biophysical properties underlying α-synuclein aggregation and toxicity.

Materials and Methods

Materials

Stock solutions of 1,2-dioleoyl-*sn*-glycero-3-phosphocholine (DOPC), 1,2-dioleoyl-*sn*-glycero-3-phosphate (DOPA), and 1-palmitoyl-2-[6-[(7-nitro-2-1,3-benzoxadiazol-4-yl)amino]hexanoyl]-sn-glycero-3-phosphocholine (NBD-PC) in chloroform were purchased from Avanti Polar Lipids, Inc. and used without further purification. 2-(N-morpholino)ethanesulfonic acid hydrate (MES hydrate), ethylenediaminetetra-acetic acid (EDTA) and phosphate-buffered saline (PBS) tablets were purchased from Sigma Chemical Co. Sodium chloride (NaCl), Sodium hydroxide (NaOH) and 4-(2-hydroxyethyl)-1-piperazineethanessulfonic acid (HEPES, Free Acid) were purchased from Mallinckrodt Chemicals. Alexa Fluor® 647 carboxylic acid, succinimidyl ester was purchased from Invitrogen. The Superdex 200 gel-filtration column was purchased from GE Healthcare Life Sciences, and the Microcon YM-100 centrifugal filter units were obtained from Millipore.

Vesicle and supported lipid bilayer preparation

Lipid stock solutions in chloroform were mixed in the appropriate molar ratios, dried under a stream of nitrogen and placed under vacuum for 1 hour. The dried lipids were rehydrated in 50 mM MES hydrate, 0.1 mM EDTA, and 250 mM NaCl buffer, pH 5.0 adjusted with concentrated NaOH. Large unilamellar vesicles were prepared by extruding 21 times through 50 nm polycarbonate membranes. The vesicle solution was then centrifuged for 5 minutes at 14,000 rpm (Eppendorf Minispin Plus). The vesicles were stored at room temperature and shielded from light. Supported lipid bilayers were formed by vesicle fusion inside a 60 μl perfusion chamber (Invitrogen Inc.) on appropriately treated glass slides. After 5 minutes, excess vesicles were removed from the perfusion chamber using the same buffer used in vesicle preparation. Glass coverslips were washed in ICN 7X detergent (MP Biomedicals), rinsed profusely in DI water, dried with a stream of nitrogen, and baked at 450 °C for 4 hours. The slides and vesicles were used within a day of preparation. For experiments at pH 5.0, the buffer solution of 50 mM MES hydrate, 0.1 mM EDTA, and 250 mM NaCl buffer, pH 5.0 was exchanged with 50 mM MES hydrate, 0.1 mM EDTA, and 100 mM NaCl buffer, pH 5.0. For pH 7.4 experiments, the buffer solution was further exchanged with 50 mM HEPES, 0.1 mM EDTA, and 100 mM NaCl buffer, pH 7.4 adjusted with concentrated NaOH. At least 5 mL of buffer was passed through the perfusion chamber to ensure complete exchange.

Expression, Purification and Labeling of α-synuclein

The protein was expressed in *E. Coli* and purified as described previously.[25] The protein was preferentially labeled at the N-terminus: monomeric α-synuclein (0.56 mM in 225 μL PBS, pH 7.0) was mixed with Alexa Fluor 647 carboxylic acid, succinimidyl ester (0.25 mg in 25.0 μL dimethyl sulfoxide (DMSO)). The mixture was placed on a Microplate shaker at 800 rpm for 2 hours. The protein solution was then loaded onto a Superdex 200 gel-filtration column and eluted in 50 mM HEPES, pH 7.4. The protein concentration and degree of labeling were determined using UV-vis absorbance measurements (the degree of labeling of the protein is typically 20%, mol/mol). The protein was then aliquoted and stored at −20° C.

α-Synuclein incubation

Prior to each experiment an aliquot was thawed and centrifuged through a Microcon YM-100 centrifugal filter unit with a molecular-weight cutoff of 100 kDa to remove any aggregates. For binding experiments at pH 5.0, the concentrated protein eluted in HEPES, pH 7.4 was diluted 100 fold in MES buffer at pH 5.0 and used immediately. The pH of the protein solution was checked prior to each experiment. In all experiments the protein was incubated for 20 minutes. For pH 5.0 the incubation and rinsing buffer contained: 100 mM NaCl, 0.1 mM EDTA and 50 mM MES. For pH 7.4 the incubation and rinsing buffer contained: 100 mM NaCl, 0.1 mM EDTA and 50 mM HEPES.

pH Shift experiments

To switch the pH 3 mL of solution was exchanged. To switch to pH 5.0 a 100 mM NaCl, 0.1 mM EDTA, 50 mM MES buffer was used. To switch to pH 7.4 a 100 mM NaCl, 0.1 mM EDTA, 50 mM HEPES buffer was used.

Imaging of supported lipid bilayers

A Nikon TE2000 fluorescence microscope equipped with either a Cascade 512B or a Cascade 650 CCD camera (Roper Scientific) was used to image the bilayers. An X-Cite 120 arc lamp (EXFO) was used as a light source. The NBD and Alexa fluorophores were imaged using NBD and Alexa Fluor 647 filter sets, respectively (Chroma Technology Corp.). Figure S1C was acquired using a 100X, 1.30 NA objective. The rest of the Images were acquired using a 40X, 1.30 NA objective. All the images were acquired in the same spot, and excess protein was removed before imaging.

Image Quantification

For all reported quantification, e.g. integrated intensities and line scans, appropriate backgrounds (dark noise of the camera, glass auto fluorescence, etc) are subtracted off using counts obtained from a fluorophore-free bilayer. To determine the amount of protein adsorbed representative areas were selected and the total intensity in those areas was determined. To determine the percent area coverage and the NBD depletion the following methods were used: Raw images are cropped to 160 μm × 160 μm and thresholded using a MatLab script. The threshold limit is set such that the PA-rich regions are below, while the PC-rich regions are above the limit. To calculate the percent area coverage of PA-rich regions, the number of pixels whose intensity is less than the threshold limit are summed and divided by the total number of pixels in the image. To calculate the percent NBD depletion, the average intensities of all the pixels below the threshold limit (PA-rich regions) and above the threshold limit (PC-rich regions) respectively are used.

Results and Discussion

Formation of supported lipid bilayers

The lipid composition used in this study was 30 mol% DOPA/69 mol% DOPC/1 mol% tail-labeled NBD-PC, unless otherwise noted. Supported lipid bilayers were formed by vesicle fusion in a buffer containing 250 mM NaCl (pH 5.0). The ionic strength of the bulk solution was then reduced to 100 mM NaCl at either pH 5.0 or pH 7.4. Under these conditions, the bilayer was uniformly mixed and fluid.

α-Synuclein adsorption at pH 6.0 and 7.4

In a first series of experiments we characterized the binding of Alexa Fluor 647–labeled α-synuclein to the bilayer at a pH of 5.0. Prior to protein addition, the bilayer was uniformly mixed (not shown). Figure 1A–C and Figure 1D–F show the bilayer and protein,

respectively. Aliquots of α-synuclein were added sequentially to the bilayer at the following concentrations: 0.26 μM (Figure 1A,D), 1.04 μM (not shown), 1.3 μM (Figure 1B,E) and 1.3 μM (Figure 1C,F). After each incubation step, the solution was exchanged with fresh buffer, and fluorescence microscopy images were acquired at the same spot on the bilayers. In the bilayer images, Figure 1A–C, the presence of dark and bright regions indicates that, as a result of protein addition, the lipids have phase separated. The dark regions in the bilayer images correspond with regions of enhanced adsorption in the protein images, Figure 1D–F. This observation coupled with the fact that the labeled lipid was PC allows us to assign the dark regions as PA-rich and the bright regions as PC-rich. The extent of depletion of the NBD fluorophore (attached to the tail of a PC lipid) from the dark regions was ~20% (Figure 1A–C). Photobleaching experiments confirmed that the bilayer was continuous and fluid across the whole surface before and after the lipids de-mixed (Supporting Information, Figure 1), implying that the observed phase separation was fluid-fluid. The first application of protein took the membrane from a mixed to a de-mixed state. The area fraction of the PA-rich regions increased with the next two applications of protein (not shown and Figure 1B), whereas the last application resulted in no further de-mixing (Figure 1C). A characteristic feature of the protein images was the presence of small black dots corresponding to areas of low protein adsoption (Figure 1D–F). High magnification images (Supporting Information, Figure 2C) showed that the dots correspond with the location of caps in the bilayer.[50]

To monitor protein binding we determined the total intensity of the Alexa 647 fluorophore at three areas on the surface. The bilayer in region 1 switched from being PC-rich to PA-rich from Figure 1A (application of 0.26 μM α-synuclein) to Figure 1B (application of 1.04 and 1.3 μM α-synuclein). In contrast, the bilayer was PA-rich in region 2 and PC-rich in region 3 immediately after first adding α-synuclein and remained unchanged throughout the experiment (Figure 1A–C). Region 1 was the only region to show an increase in protein adsorption throughout all four applications of protein: an increase of ~3.5-fold was observed from Figure 1D (application of 0.26 μM) to Figure 1E (application of 1.04 and 1.3 μM), and an increase of ~1.2-fold was observed from Figure 1E to Figure 1F (application of 1.3 μM). In regions 2 and 3 the amount of protein bound increased ~2.5-fold and ~2.3-fold respectively from the first application (Figure 1D) to the third application (Figure 1E), whereas the amount of bound protein did not increase after the last addition of protein (Figure 1F). Binding did not saturate on the entirety of the PA-rich region, but it did saturate on the PC-rich regions.

The membrane lipids also reorganized into PA-rich and PC-rich regions when α-synuclein was added to the bilayer at pH 7.4 (Figure 2 A–C). In this case, the bilayer was incubated with α-synuclein at 0.26 μM (Figure 2A,D), 1.04 μM(not shown), 1.3 μM (Figure 2B,E), 1.3 μM (not shown), and 1.3 μM (Figure 2C,F). Images were acquired at the same spot after the bulk solution was exchanged with buffer. As observed at pH 5.0, the area fraction of the PA-rich regions increased with increasing protein concentration. The extent of depletion of the NBD fluorophore from the PA-rich regions was ~23% (Figure 2A–C). The adsorption of α-synuclein to the bilayer was monitored by measuring changes in the average intensity of Alexa Fluor 647 in two regions (highlighted in Figure 2D–F). Region 1, which was PA-rich immediately after first adding α-synuclein and remained PA-rich throughout the experiment (Figure 2A–C), exhibited a ~1.2-fold increase in protein intensity from Figure 2D (application of 0.26 μM) to Figure 2E (application of 1.04 μM and 1.3 μM) and a ~1.1-fold increase from Figure 2E to Figure 2F (two applications of 1.3 μM). Region 2, which was PC-rich immediately after the first addition of α-synuclein and remained PC-rich throughout the experiment (Figure 2A–C), exhibited a ~1.8-fold increase in protein intensity from Figure 2D to Figure 2E and no change in protein intensity from Figure 2E to Figure 2F.

Similar PC- and PA-rich regions were formed upon α-synuclein binding at pH 5.0 and 7.4 regardless of whether the protein was added sequentially or all at once (Supporting Information, Figure 2, Figure 3). This result implies that the same or a similar thermodynamic endpoint is achieved in each case. In general, the lipid separation occurred more rapidly at pH 5.0 (~3 minutes) than at pH 7.4 (~10 minutes). The data in Figure 1 and Figure 2 reveal the following salient trends: (i) protein binding increases with increasing α-synuclein concentration; (ii) more α-synuclein binds to the PA-rich regions than PC-rich regions, and the binding to each region is greater at pH 5.0 than pH 7.4 (see also Figure 5); (iii) protein binding saturates on the PC-rich regions but not the PA-rich regions; (iv) the morphology of the PA-rich regions is more extended and branched at pH 5.0 than 7.4, perhaps because more rapid lipid separation occurs at the lower pH; and (v) for a given α-synuclein concentration the area fraction of the PA-rich region is greater at pH 5.0 than 7.4. Approximately 20 mol% of the protein was labeled on the N-terminus (see Materials and Methods). Repeating the above experiments with unlabeled protein resulted in the same observations regarding the bilayer response to protein adsorption.

One explanation for the observed lipid reorganization on the PA-PC bilayer may be that an enrichment of anionic lipids neutralizes the positive charges on the surface of the membrane bound protein. Structural studies of α-synuclein in the presence of anionic detergents or phospholipids indicate that the protein adopts an α-helical structure upon binding to membranes.[11−15] In this conformation the protein's lysine residues flank the hydrophobic face of the helix at the polar-nonpolar interface, whereas the acidic residues (aspartates and glutamates) are solvent-exposed on the hydrophilic face. The C-terminal region (spanning residues ~100–140) is highly negatively charged at pH 7.4, but only moderately so at pH 5. Because the α-helix is ~15 nm long and 1 nm wide,[52] the charge density of the membrane-exposed face is ~0.8/nm^2 (corresponding to 12 lysines/helix). For the lipid mixture used in our study (30 mol% DOPA/70 mol% DOPC), the surface area per lipid is estimated to be 0.72 nm^2 (the radius of DOPC is 4.5 Å;[53] to estimate packing density we use a hexagonal close-packed model). A study of DOPA in DOPC revealed that pK_{a1} is approximately equal to 3.2 and pK_{a2} is approximately equal to 7.9.[48] Accordingly, the average charge of the PA lipids at pH 5.0 and 7.4 is (-)0.99 and (-)1.2 respectively. The charge densities are then calculated to be 0.41/nm^2(pH 5.0) and 0.52/nm^2 (pH 7.4), given that 30% of the lipids are ionizable. Because these charge densities are less than that of the membrane-exposed face of helical α-synuclein, we infer that the lipids reorganize to satisfy the condition of charge neutralization.[54] Due to the lower membrane charge density at pH 5.0, as compared with pH 7.4, there is a larger driving force for reorganization at pH 5.0. This may be a contributing factor to the observation that a larger area fraction of PA-rich regions is observed at pH 5.0 than 7.4.

The requirement to neutralize positive charges on the surface of helical α-synuclein has also been suggested to drive lipid reorganization upon binding of the protein to a PG-PC bilayer.[39] In this case, 40 mol% anionic lipid and 2.6 μM protein were required to observe lipid phase separation, whereas 30 mol% anionic lipid and 0.26 μM protein were sufficient to induce lipid reorganization in the PA-PC bilayers described here. PC and PG are known to mix well.[55,56] In contrast, PA and PC readily separate when PA is protonated[49,51] or when Ca^{2+}-PA^{2-} complexes are generated.[51,57] Thus, lipid de-mixing is likely to be a key driving force in the reorganization of lipids induced by α-synuclein in PA-PC bilayers,[54,58] in addition to charge neutralization. At pH 7.4 a substantial minority of PA^{2-} is present; at pH 5.0 the PA is almost entirely PA^{1-}. The increased charge-charge repulsion between the (2−) species results in a stronger drive for lipid-lipid mixing at pH 7.4 than 5.0. This may be a contributing factor to the observation that a smaller area fraction of PA-rich regions is observed at pH 7.4 than 5.0.

When 0.26 μM α-synuclein is added, there is one protein for every 10 lipids. If the N-terminus is fully helical, and the C-terminus does not adsorb, then one protein covers, at a minimum, the area of ~21 lipids (when helical the N-terminus is ~15 nm long and ~1 nm wide;[52] as discussed above the surface area per lipid is estimated to be ~0.72 nm^2.) A more extended conformation would cover more lipids per protein. For each addition of protein in Figure 1 and Figure 2, multiple monolayer equivalents of protein are introduced. Due to limitations inherent in fluorescence microscopy the amount of protein which adsorbs after each addition has not been absolutely quantified (changes can easily be quantified, but not absolute amounts). That the protein continues to adsorb on the PA-rich regions with each addition strongly suggests that multilayer adsorption is occurring at these sites. The helical content of membrane-bound α-synuclein increases with increasing anionic lipid content.[59] If residues 1–94 are fully helical several hydrophobic residues are solvent exposed ('solvated'): Met 5, Val 16, Leu 38, Val 49, Val 71, Val 82, and Phe 94.11،36 Multilayer adsorption would reduce the free energy of the system by burying the exposed residues.39

The pI of α-synuclein is 4.7.[60] Therefore, the protein has a net charge of almost zero at pH 5.0 and an overall negative charge at pH 7.4. As the pH is lowered the protein adopts a slightly more extended conformation in solution.[61,62] In executing the experiments for Figure 1 and Figure 2 it was observed that lipid de-mixing proceeded more slowly at pH 7.4 (~10 minutes) than pH 5.0 (~3 minutes). When the solution phase protein encounters the membrane-bound protein it may be repelled due to charge-charge repulsion. This will be more likely to occur at pH 7.4 than 5.0, reducing the adsorption rate and slowing the consequent de-mixing. The fact that the morphology of the PA-rich domains varies with pH may also be determined by the different charge states of the protein: more highly charged, slower de-mixing, reduced branching.

In Figure 1 and Figure 2 the amount of protein adsorbed is observed to vary amongst the different regions: PA-rich (pH 5.0), PA-rich (pH 7.4), PC-rich (pH 5.0) and PC-rich (pH 7.4) (highest binding to lowest binding). This observation, coupled, with (a) the knowledge that α-synuclein has different charge states at the two pHs and (b) the observation that α-synuclein structure varies with anionic lipid content,[59] suggests that α-synuclein binds to these regions in different ways.

Effect of switching pH on lipid separation and protein adsorption

In the next phase of our study, we investigated how the protein-rich regions formed at pH 5.0 differ from those formed at pH 7.4. To address this question, α-synuclein was added to the bilayer at one pH, and subsequent protein binding was monitored after switching to the other pH (Figure 3, Figure 4). At all times 100 mM NaCl was present.

A PA/PC bilayer was incubated with 0.26 μM α-synuclein at pH 5.0 (Figure 3A,E) or pH 7.4 (Figure 4A,E). The lipids re-organized into PA-rich regions (e.g. region 1) and PC-rich regions (e.g. region 2), and protein bound preferentially to the PA-rich regions. The pH was then switched from 5.0 to 7.4 (Figure 3B,F) or from 7.4 to 5.0 (Figure 4B,F). The extent of protein adsorption is plotted in Figure 5; the data points represent the average of 12 individual experiments. Of note: (i) More protein bound at pH 5.0 as compared to pH 7.4. (ii) No loss of protein was observed when the pH was decreased from 7.4 to 5.0. (iii) A significant loss of protein was observed when the pH was increased from 5.0 to 7.4. The observed desorption upon raising the pH can be attributed to charge-charge repulsion, given that the C-terminus is near neutral at pH 5.0 but highly anionic at pH 7.4.

After the pH was switched, the bilayers were incubated with the following concentrations of α-synuclein at the new pH: 1.3 μM (pH 7.4: Figure 3C,G; pH 5.0: Figure 4C,G) and 2.6 μM (pH 7.4 Figure 3D,H; pH 5.0: Figure 4D,H). In both cases growth of new PA-rich regions

was observed (e.g. region 3). Figure 5 plots the amount of protein adsorption after each incubation in newly created PA-rich regions, original PA-rich regions, and PC-rich regions. It can clearly be seen that in both cases the greatest adsorption occurred on the newly-created PA-rich region.

The structure of membrane-bound α-synuclein depends on the anionic lipid content.[59] Consequently, we expect that the membrane-bound protein is more helical at pH 7.4 than 5.0 and furthermore that more hydrophobic residues are solvated at pH 7.4 than 5.0.[39] After the pH switch and further addition of protein there are three different membrane/protein interfaces, schematically illustrated in Figure 6: (i) PC-rich: lowest membrane charge density, membrane-bound protein least helical, lowest density of solvated hydrophobic residues. (ii) PA-rich formed at pH 7.4: highest membrane charge density, membrane bound protein most helical, highest density of solvated hydrophobic residues. (iii) PA-rich formed at pH 5.0: properties closer to (ii) than (i).

When the pH is switched it might be expected that there would be concomitant changes in the PA charge and the structure of the membrane-bound protein. That protein does not adsorb equally to the two PA-rich regions (i.e. the initial and new regions) in Figure 3 and Figure 4 indicates that the structure of the membrane-bound protein does not fully convert. The possibility that it partially converts is left open. As to the charge on the PA lipids we cannot make direct observations, but note that the presence of membrane-bound protein will have a strong local effect on the lipid charge.[63] The lack of full conversion of the membrane-bound protein means that in those regions the charge on the PA is unlikely to adjust fully. It is also possible that the local electrostatic environment prevents the protein from fully adjusting its charge when the pH is switched. As the C-terminus is not significantly involved in the adsorption process the charge on this region is expected to adjust to a greater degree than that on the rest of the protein.

On the PA-rich regions there is multilayer adsorption. The preference for the favored site for protein-protein contacts depends on the solution pH: At pH 7.4 protein-protein contacts are favored on the PA-rich regions formed at pH 7.4. At pH 5.0 protein-protein contacts are favored on the PA-rich regions formed at pH 5.0. Possible explanations for why different binding sites are preferred, depending on the solution pH, are discussed below.

We begin by examining the thermodynamics of the system. Upon adsorbing to the membrane the protein loses much of its configurational entropy, increasing the system free energy; the amount of loss depends on the degree of protein structure adopted upon adsorption. As α-synuclein is a charged molecule electrostatic repulsion may also occur upon adsorption, further increasing the system free energy; this is likely to be a significant consideration at pH 7.4 where the C-terminus is highly negatively charged (15 of 40 residues are acidic). These increases in the system free energy may be offset by a number of factors, e.g. increase in configurational entropy of associated water molecules, favorable electrostatic interactions, favorable van der Waals interactions, burial of exposed hydrophobic residues on the membrane-bound protein. In this context the membrane-bound protein on the two PA-rich regions is examined: Protein adsorbing on the PA-rich regions formed at pH 7.4 gives up a greater degree of configurational entropy and buries more exposed hydrophobic residues than the protein adsorbing on the PA-rich regions formed at pH 5.0. A consideration of the fact that at pH 7.4 the C-terminus is highly charged, while at pH 5.0 it is near neutral, allows us to see how the adsorption free energy landscape could shift to prefer one site over the other: Comparing the two adsorption sites we see that the PA-rich region formed at pH 7.4 is a more highly ordered surface (due to the presence of bound α-synuclein with a high degree of α-helical structure), and this order likely translates through the structures of additional molecules that adsorb to the surface. It is possible that

this increased order decreases the unfavorable (repulsive) tail-tail interactions relative to those that occur in the PA-rich region formed at pH 5.0. If so, this could shift the adsorption free energy landscape at pH 7.4 in favor of the PA-rich region formed at pH 7.4. In contrast, at pH 5.0 the neutral C-termini of neighboring molecules would no longer repel each other, but rather they could participate in favorable van der Waals interactions. This would shift the adsorption free energy landscape at pH 5.0 in favor of the PA-rich region formed at pH 5.0, as the more disordered binding in this region would bring a portion of the C-termini in closer contact than in the PA-rich region formed at pH 7.4, allowing for favorable van der Waals interactions.

Next we consider the kinetics of adsorption. Two possible kinetic barriers which may play a role in this system are examined: (i) Upon adsorption a degree of structural rearrangement may be required. If there is a significant energetic barrier to the required rearrangement, kinetics can dominate over thermodynamics. Adsorbing to the PA-rich regions formed at pH 5.0 requires less structural reorganization. If there are kinetic barriers to reorganization then it might, at first glance, appear that the PA-rich regions formed at pH 5.0 would be favored. However, the higher helical content required for adsorption on the PA-rich regions formed at pH 7.4 could have a lower kinetic barrier, if one exists, due to cooperativity. At present we do not have enough information to say whether rearrangement kinetic barriers favor one adsorption site over the other. (ii) The solution phase protein may encounter the surface in such a way that there is a strong electrostatic repulsion between the adsorbing protein and the already bound protein. This is more likely to be an issue at pH 7.4 than 5.0 and indeed we have observed that adsorption is slower at pH 7.4 than 5.0. The PA-rich regions formed at pH 5.0 are more disordered; when the pH is increased the increased negative charge on the membrane-bound protein will be smeared out across the region. At 100 mM NaCl the Debye screening length is 9.6 Å. Given that, the more discretely located membrane-bound C-termini in the PA-rich regions formed at pH 7.4 may allow more opportunity for the protein to approach the surface without encountering repulsive interactions. In this aspect there may be a kinetic discrimination for adsorption on the PA-rich regions formed pH 7.4.

At present we do not have enough information to determine the exact extent to which thermodynamics and/or kinetics control the discrimination between the two PA-rich regions. However, the fact that protein adsorption occurs quickly suggests that thermodynamics predominates.

The above discussion leads to the following predictions about the structure of the protein-protein contacts formed in the two situations: Contacts formed at pH 7.4 will be more ordered and the aggregates will be more structurally homogeneous. Contacts formed at pH 5.0 will be more varied and the aggregates will be more structurally heterogeneous.

Investigating the stability of protein-protein contacts using pH and ionic strength

We observed desorption of α-synuclein from the surface when the pH was raised from 5.0 to 7.4, but not in the reverse case. In the experiment shown in Figure 3E and 3F, the observed desorption occurred after incubating with a low protein concentration (0.26 μM). Close inspection of the images suggested that the protein did not desorb completely uniformly. However, due to the overall low signal-to-noise ratio, it was impossible to determine, within error, whether this was in fact the case. To explore further, the experiment was repeated by exposing the membrane to a higher concentration of protein (5.2 μM). Incubation of the bilayer with α-synuclein induced separation into PA-rich and PC-rich regions (Figure 7A) and preferential binding of the protein to the PA-rich regions (Figure 7C), as observed previously. Interestingly, in the regions of enhanced protein binding the α-synuclein-rich regions did not overlay exactly with the PA-rich regions. Rather, the protein-rich regions appeared morphologically less distinct (or more ‘blurred’) compared to the PA-rich regions.

Upon increasing the pH of the bulk solution to 7.4, the protein underwent non-uniform desorption (Figure 7C, D), a phenomenon underscored by the accompanying line scans (Figure 7E). The remaining bright clusters had widths of no more than a few micrometers and were thus close to the diffraction limit. An analysis of many images strongly suggested that these clusters were coincident with the interface between the PC- and PA-rich regions.

The non-uniform desorption implies that there are at least two populations of protein on the PA-rich regions. To explore further we examined the effect of changing the screening environment in addition to changing the protein charge. The bilayer was incubated with 5.2 μM α-synuclein at pH 5.0 in the presence of 100 mM NaCl (Figure 8A, E). The electrostatic environment was manipulated in three steps. First, the screening environment was altered by increasing the ionic strength from 100 to 1000 mM (Figure 8B, F); in doing so the Debye screening length decreases from 9.6 to 3 Å. This has the effect of decreasing the attractive electrostatic interactions which could lead to protein desorption. In Figure 8F, it can be seen that the protein on the PA-rich region underwent significant non-uniform desorption with bright, PA-associated clusters becoming visible on the bilayer. This effect is particularly clear in the associated line scan (Figure 8I). Second, the charge on the protein was increased by raising the pH to 7.4 (Figure 8C, G). This resulted in further protein desorption, and the non-uniformity of this desorption on the PA-rich region was even more pronounced. Third, the ionic strength was reduced to 100 mM (Figure 8D, H), thereby increasing the repulsive interactions. Further non-uniform desorption on the PA-rich region resulted.

In the previous section we argued that at pH 5.0 there can be significant flexibility in the structure of the adsorbed protein. The heterogeneity observed in Figure 8 provides strong supporting evidence for our hypothesis: the non-uniform desorption with each manipulation of the electrostatic environment argues that there are multiple populations. Populations are disrupted when (i) the attractive electrostatic interactions are reduced; (ii) the charge on the protein, particularly the C-terminus, increases; and (iii) repulsive interactions are enhanced (the Debye screening length increases from 3 Å to 9.6 Å).

We also detected the presence of at least one population of membrane-bound α-synuclein that did not undergo desorption in response to any of the alterations in solution conditions. This finding suggests that the protein in the resistant aggregates was in a deep energy minimum. Interestingly, the fluorescence intensity corresponding to this resistant population correlated with the interfaces between the PA-rich and PC-rich regions. These interfaces appeared to act as nucleation sites for the formation of more stable structures. One possible driving force that may have enabled the protein to adopt a relatively stable conformation is the line energy at the PA/PC interface (this interface is highly branched and thus has a high length-to-surface area ratio). It costs energy to maintain such a line, and, therefore, the formation of compensatory, lower energy protein structures would be favored at the interface.

At each step in Figure 8 desorption also occurred from the PC-rich regions. Within the resolution limits, desorption always occurred in a uniform manner. We previously suggested that there is ~1 monolayer coverage on PC-rich regions.[39] Uniform desorption is consistent with this suggestion: each of the steps in Figure 8 would be expected to perturb a fraction of heterogeneously bound protein, whereas the uniformity of desorption from the PC bilayer suggests that the more complex interactions found in multilayer formation did not occur in this case (to the limit of our resolution). The amount of desorption from a PC-only membrane in response to each step in Figure 8 has been quantified (Supporting Information, Figure 4).

We did not observe desorption of α-synuclein from the surface when the pH was decreased from 7.4 to 5.0 (Figure 4E, F; Figure 5). However, we observed non-uniform desorption of protein aggregates at pH 5.0 in response to an increase in ionic strength (from 100 mM to 1000 mM NaCl; Figure 8E, F). Consequently, we decided to examine the effect of ionic strength on the stability of protein-protein contacts at pH 7.4. Incubation of the bilayer with 5.2 μM α-synuclein at pH 7.4 in the presence of 100 mM NaCl resulted in separation of the PA and PC lipids (Figure 9A) and preferential binding of the protein to the PA-rich domains (Figure 9D). When the NaCl concentration was increased from 100 mM to 1000 mM, a fraction of the protein was observed to desorb uniformly from both PA-rich and PC-rich regions (Figure 9B, E). The uniformity of this desorption was markedly evident in the associated line-scans (Figure 9G). A larger fraction, ~24%, desorbed from the PA-rich region than the PC-rich region, ~15%.

A decrease in the NaCl concentration from 1000 mM to 10 mM led to the formation of new PA-rich domains and light-colored ring structures (Figure 9C). We have previously observed separation in PA/PC bilayers when the salt concentration is reduced below 100 mM.[49] This separation arises because the $PA^{1-/2-}$ in the PC-rich region protonates to form PA°, which is not miscible with PC above a threshold value. The rings in Figure 9C are three dimensional structures (referred to as 'caps') that appear when the bilayer is exposed to an asymmetric screening environment.[50] Interestingly, the data in Figure 9F reveal no loss of α-synuclein from the protein clusters but some migration of protein to the new PA-rich regions, possibly from the edges of the pre-existing aggregates. Although α-synuclein preferentially binds to membranes enriched in anionic lipids, it can also bind to PA°-rich regions, thereby most likely "recharging" the PA.[49]

Interestingly, the decrease in ionic strength from 1000 to 10 mM (Debye screening length increased from 3 to 30 Å) had no effect except to induce the spreading of a small fraction of the protein. It follows that the membrane-bound protein at pH 7.4 is packed in such a way as to minimize repulsion between the highly charged C-termini. This observation and the overall lack of desorption strongly suggests that the α-synuclein aggregates have a high degree of order, providing further supporting evidence for our hypothesis that the membrane bound protein is more helical at pH 7.4. Highly helical membrane-bound protein presents a smaller variety of possible protein-protein contact points. This restriction on the number of interaction sites coupled with the constraint placed on adsorption by the highly charged C-terminus implies that there are few possible configurations in which protein-protein contacts can be formed. There is in effect a high degree of selectivity, leading to a high degree of structure and stability. The uniformity of protein loss upon increasing the ionic strength (Figure 9D, E, G) can be attributed to packing effects: As layers of helical protein adsorb on top of each other, packing faults are likely to accumulate (each layer packs less perfectly than the previous layer). Thus, the protein at the top is less stable than the protein at the bottom. At 1000 mM NaCl there is still a substantial amount of the protein bound to the membrane, whereas if we incubate a bilayer with protein at high ionic strength, comparatively little protein adsorbs. As discussed in our previous work,[39] this hysteresis in the binding-unbinding transition underscores the role that hydrophobic residues play in the lipid-protein and protein-protein interactions.

Effect of lipid-protein interactions on protein-protein interactions

The results of this paper suggest that the structure of the membrane-bound protein plays a key role in controlling the structure of the subsequent aggregate formation. To explore further, the following experiment was conducted (Figure 10; only protein images are shown): A PA/PC bilayer was incubated with 0.26 μM α-synuclein at pH 7.4 in the presence of 100 mM NaCl (Figure 10A). No change was observed when the pH of the bulk solution was decreased to 5.0 (Figure 10B). Incubation of the bilayer with 2.3 μM α-synuclein

induced new separation and increased protein binding (Figure 10C). The net amount of protein bound to pre-existing aggregates was less than that bound to the new PA clusters, consistent with observations from Figure 4 and Figure 5. Upon increasing the pH of the bulk solution to 7.4 (Figure 10D), non-uniform desorption was observed from the new aggregates that had formed at pH 5.0, while uniform desorption was observed from the original PA-rich-protein template (formed at pH 7.4 in the presence of 0.26 μM α-synuclein). This experiment highlights that it is possible for α-synuclein to adopt a variety of membrane-bound structures, depending on the solution condition during adsorption, and that both ordered and disordered aggregates may be formed on the same surface.

Conclusions

In this paper we have shown that: (i) The charge distribution of both the membrane and the protein affects the amount of protein which adsorbs. (ii) The charge distribution of both the membrane and protein affects the structure of both the membrane-bound protein and the protein aggregates. (iii) Protein can be desorbed by either reducing the attractive electrostatic interactions and/or increasing the repulsive electrostatic interactions. Conditions under which complete desorption occurs have not been elucidated, highlighting the role of hydrophobic interactions.[39] (iv) The degree of structural heterogeneity in the adsorbed protein depends on the conditions under which it bound the membrane.

Protein aggregation may cause toxicity by removing proteins required for normal cellular function and/or by forming specific assemblies which disrupt cellular processes. In this paper we have shown that a variety of different end results, e.g. different degrees of aggregation, different aggregate structures, can be achieved by varying the environmental conditions, particularly the charge on the membrane and protein. It is known that with aging membrane charge changes: the brains of aged rats have elevated levels of phosphatidic acid,[64] and the ratio of anionic to zwitterionic phospholipids increases in the brains of PD patients.[65] Our observation that α-synuclein forms a multitude of membrane-bound aggregates of unknown toxicities has considerable implications for drug design, as it suggests that single molecules may not be effective in mitigating α-synuclein-mediated neurodegeneration. Instead, cocktails of drugs or other creative routes may be necessary.

Supplementary Material

Refer to Web version on PubMed Central for supplementary material.

Acknowledgments

This work was supported by NIH grant R01 NS049221 (J.-C.R. and J.S.H.) and awards from the Showalter Trust (J.S.H. and J.-C.R.) and the Department of Energy (DE-FG02-08ER64579) (J.-C. R.). The authors thank Jagadish Hindupur and John Hulleman for assistance with α-synuclein expression, purification and labeling.

References

1. Rochet JC. Expert Rev Mol Med 2007;9:1. [PubMed: 17597554]
2. Selkoe DJ. Nature 2003;426:900. [PubMed: 14685251]
3. Clayton DF, George JM. J Neurosci Res 1999;58:120. [PubMed: 10491577]
4. Iwai A, Masliah E, Yoshimoto M, Ge NF, Flanagan L, Desilva HAR, Kittel A, Saitoh T. Neuron 1995;14:467. [PubMed: 7857654]
5. Maroteaux L, Scheller RH. Brain Res Mol Brain Res 1991;11:335. [PubMed: 1661825]
6. Cabin DE, Shimazu K, Murphy D, Cole NB, Gottschalk W, McIlwain KL, Orrison B, Chen A, Ellis CE, Paylor R, Lu B, Nussbaum RL. J Neurosci 2002;22:8797. [PubMed: 12388586]

7. Murphy DD, Rueter SM, Trojanowski JQ, Lee VMY. J Neurosci 2000;20:3214. [PubMed: 10777786]
8. Sidhu A, Wersinger C, Vernier P. FEBS Letters 2004;565:1. [PubMed: 15135042]
9. Weinreb PH, Zhen WG, Poon AW, Conway KA, Lansbury PT. Biochemistry 1996;35:13709. [PubMed: 8901511]
10. Davidson WS, Jonas A, Clayton DF, George JM. J Biol Chem 1998;273:9443. [PubMed: 9545270]
11. Bussell R Jr, Eliezer D. J Mol Biol 2003;329:763. [PubMed: 12787676]
12. Chandra S, Chen XC, Rizo J, Jahn R, Sudhof TC. J Biol Chem 2003;278:15313. [PubMed: 12586824]
13. Jao CC, Der-Sarkissian A, Chen J, Langen R. Proc Natl Acad Sci 2004;101:8331. [PubMed: 15155902]
14. Bisaglia M, Tessari I, Pinato L, Bellanda M, Giraudo S, Fasano M, Bergantino E, Bubacco L, Mammi S. Biochemistry 2005;44:329. [PubMed: 15628875]
15. Ulmer TS, Bax A. J Biol Chem 2005;280:43179. [PubMed: 16166095]
16. Giasson BI, Murray IVJ, Trojanowski JQ, Lee VMY. J Biol Chem 2001;276:2380. [PubMed: 11060312]
17. Han H, Weinreb PH, Lansbury PT Jr. Chem Biol 1995;2:163. [PubMed: 9383418]
18. Chiti F, Dobson CM. Annu Rev Biochem 2006;75:333. [PubMed: 16756495]
19. Baba M, Nakajo S, Tu P-H, Tomita T, Nakaya K, Lee VM-Y, Trojanowski JQ, Iwatsubo T. Am J Pathol 1998;152:879. [PubMed: 9546347]
20. Conway KA, Harper JD, Lansbury PT Jr. Biochemistry 2000;39:2552. [PubMed: 10704204]
21. Spillantini MG, Crowther RA, Jakes R, Hasegawa M, Goedert M. Proc Natl Acad Sci 1998;95:6469. [PubMed: 9600990]
22. Wakabayashi K, Matsumoto K, Takayama K, Yoshimoto M, Takahashi H. Neurosci Lett 1997;239:45. [PubMed: 9547168]
23. Conway KA, Lee S-J, Rochet J-C, Ding TT, Williamson RE, Lansbury PT Jr. Proc. Natl. Acad. Sci. U.S.A 2000;97:571. [PubMed: 10639120]
24. Conway KA, Rochet J-C, Bieganski RM, Lansbury PT Jr. Science 2001;294:1346. [PubMed: 11701929]
25. Rochet JC, Conway KA, Lansbury PT Jr. Biochemistry 2000;39:10619. [PubMed: 10978144]
26. Volles MJ, Lee SJ, Rochet JC, Shtilerman MD, Ding TT, Kessler JC, Lansbury PT Jr. Biochemistry 2001;40:7812. [PubMed: 11425308]
27. Cole NB, Murphy DD, Grider T, Rueter S, Brasaemle D, Nussbaum RL. J Biol Chem 2002;277:6344. [PubMed: 11744721]
28. Lee H-J, Choi C, Lee S-J. J Biol Chem 2002;277:671. [PubMed: 11679584]
29. Perrin RJ, Woods WS, Clayton DF, George JM. J Biol Chem 2001;276:41958. [PubMed: 11553616]
30. Necula M, Chirita CN, Kuret J. J Biol Chem 2003;278:46674. [PubMed: 14506232]
31. Zhu M, Fink AL. J Biol Chem 2003;278:16873. [PubMed: 12621030]
32. Zhu M, Li J, Fink AL. J Biol Chem 2003;278:40186. [PubMed: 12885775]
33. Rochet JC, Outeiro TF, Conway KA, Ding TT, Volles MJ, Lashuel HA, Bieganski RM, Lindquist SL, Lansbury PT. J Mol Neurosci 2004;23:23. [PubMed: 15126689]
34. Rochet, J-C.; Schieler, JL. The use of cell-free systems to characterize Parkinson's disease-related gene products. In: Nass, R.; Przedborski, S., editors. Parkinson's Disease: Molecular and Therapeutic Insights from Model Systems. San Diego, CA: Elsevier; 2008. p. 597
35. Abedini A, Raleigh DP. Phys Biol 2009;6:15005.
36. Mihajlovic M, Lazaridis T. Proteins 2008;70:761. [PubMed: 17729279]
37. Ramakrishnan M, Jensen PH, Marsh D. Biochemistry 2006;45:3386. [PubMed: 16519533]
38. Tamamizu-Kato S, Kosaraju MG, Kato H, Raussens V, Ruysschaert JM, Narayanaswami V. Biochemistry 2006;45:10947. [PubMed: 16953580]
39. Pandey AP, Haque F, Rochet J-C, Hovis JS. Biophys J 2008;96:540. [PubMed: 19167303]

40. Munishkina LA, Phelan C, Uversky VN, Fink AL. Biochemistry 2003;42:2720. [PubMed: 12614167]
41. Cuervo AM, Stefanis L, Fredenburg R, Lansbury PT, Sulzer D. Science 2004;305:1292. [PubMed: 15333840]
42. Snyder H, Mensah K, Theisler C, Lee J, Matouschek A, Wolozin B. J Biol Chem 2003;278:11753. [PubMed: 12551928]
43. Lindersson E, Beedholm R, Hojrup P, Moos T, Gai W, Hendil KB, Jensen PH. J Biol Chem 2004;279:12924. [PubMed: 14711827]
44. Emmanouilidou E, Stefanis L, Vekrellis K. Neurobiol Aging. 2008
45. Ahn BH, Rhim H, Kim SY, Sung YM, Lee MY, Choi JY, Wolozin B, Chang JS, Lee YH, Kwon TK, Chung KC, Yoon SH, Hahn SJ, Kim MS, Jo YH, Min DS. J Biol Chem 2002;277:12334. [PubMed: 11821392]
46. Jenco JM, Rawlingson A, Daniels B, Morris AJ. Biochemistry 1998;37:4901. [PubMed: 9538008]
47. Wagner K, Brezesinski G. Biophys J 2007;93:2373. [PubMed: 17557794]
48. Kooijman EE, Carter KM, van Laar EG, Chupin V, Burger KN, de Kruijff B. Biochemistry 2005;44:17007. [PubMed: 16363814]
49. Cambrea LR, Haque F, Schieler JL, Rochet JC, Hovis JS. Biophys J 2007;93:1630. [PubMed: 17483164]
50. Cambrea LR, Hovis JS. Biophys J 2007;92:3587. [PubMed: 17325003]
51. Lamberson ER, Cambrea LR, Rochet J-C, Hovis JS. J Phys Chem B 2009;113:3431. [PubMed: 19243147]
52. Rhoades E, Ramlall TF, Webb WW, Eliezer D. Biophys J 2006;90:4692. [PubMed: 16581836]
53. Kucerka N, Tristram-Nagle S, Nagle JF. J Membrane Biol 2006;208:193. [PubMed: 16604469]
54. Mbamala EC, Ben-Shaul A, May S. Biophys J 2005;88:1702. [PubMed: 15626713]
55. Findlay EJ, Barton PG. Biochemistry 1978;17:2400. [PubMed: 678517]
56. Garidel P, Johann C, Mennicke L, Blume A. Eur. Biophys. J 1997;26:447.
57. Lamberson ER, Cambrea LR, Hovis JS. J Phys Chem B 2007;111:13664. [PubMed: 18001085]
58. May S, Harries D, Ben-Shaul A. Biophys J 2000;79:1747. [PubMed: 11023883]
59. Zakharov SD, Hulleman JD, Dutseva EA, Antonenko YN, Rochet JC, Cramer WA. Biochemistry 2007;46:14369. [PubMed: 18031063]
60. Hoyer W, Antony T, Cherny D, Heim G, Jovin TM, Subramaniam V. J Mol Biol 2002;322:383. [PubMed: 12217698]
61. McClendon S, Rospigliosi CC, Eliezer D. Protein Sci 2009;18:1531. [PubMed: 19475665]
62. Wu KP, Weinstock DS, Narayanan C, Levy RM, Baum J. J Mol Biol 2009;391:784. [PubMed: 19576220]
63. Kooijman E, Tieleman D, Testerink C, Munnik T, Rijkers D, Burger K, Kruijff Bd. J. Biol. Chem 2007;282:11356. [PubMed: 17277311]
64. Giusto NM, Salvador GA, Castagnet PI, Pasquare SJ, Ilincheta de Boschero MG. Neurochem Res 2002;27:1513. [PubMed: 12512956]
65. Riekkinen P, Rinne UK, Pelliniemi TT, Sonninen V. Arch Neurol 1975;32:25. [PubMed: 1115656]

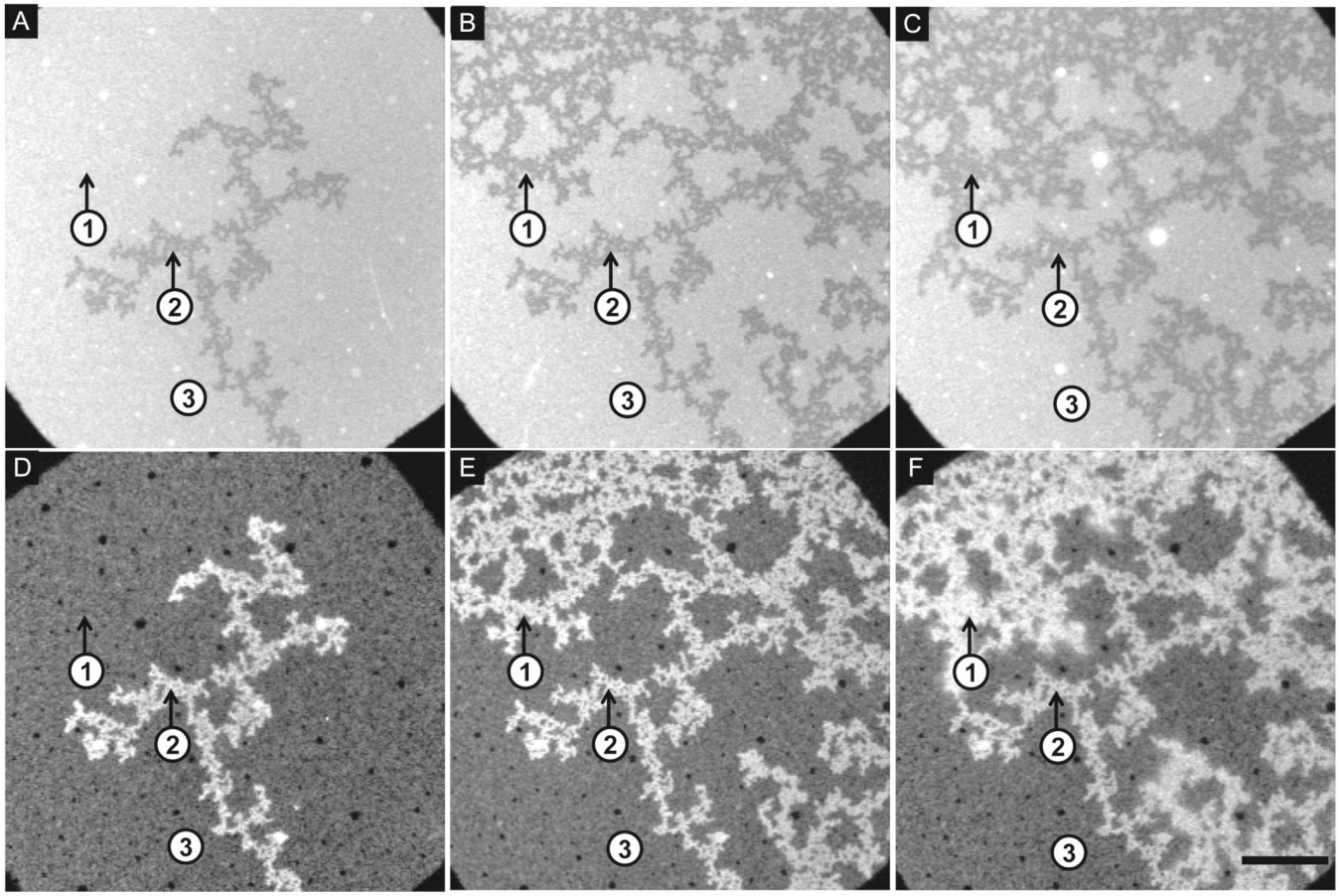

Figure 1.
Sequential addition of α-synuclein to a PA/PC bilayer at pH 5.0: Epi-fluorescence images of a 30 mol% DOPA/69 mol% DOPC/1 mol% NBD-PC bilayer at pH 5.0, 100 mM NaCl. Lipid bilayers (A–C) and corresponding protein images (D–F) are shown after successive additions of protein at 0.26 μm (A, D), 1.04 μm (not shown), 1.3 μm (B, E) and 1.3 μm (C, F). Three regions are highlighted: Region 1 (initially PC-rich, then PA-rich); Region 2 (PA-rich); Region 3 (PC-rich). The scale bar represents 40 μm.

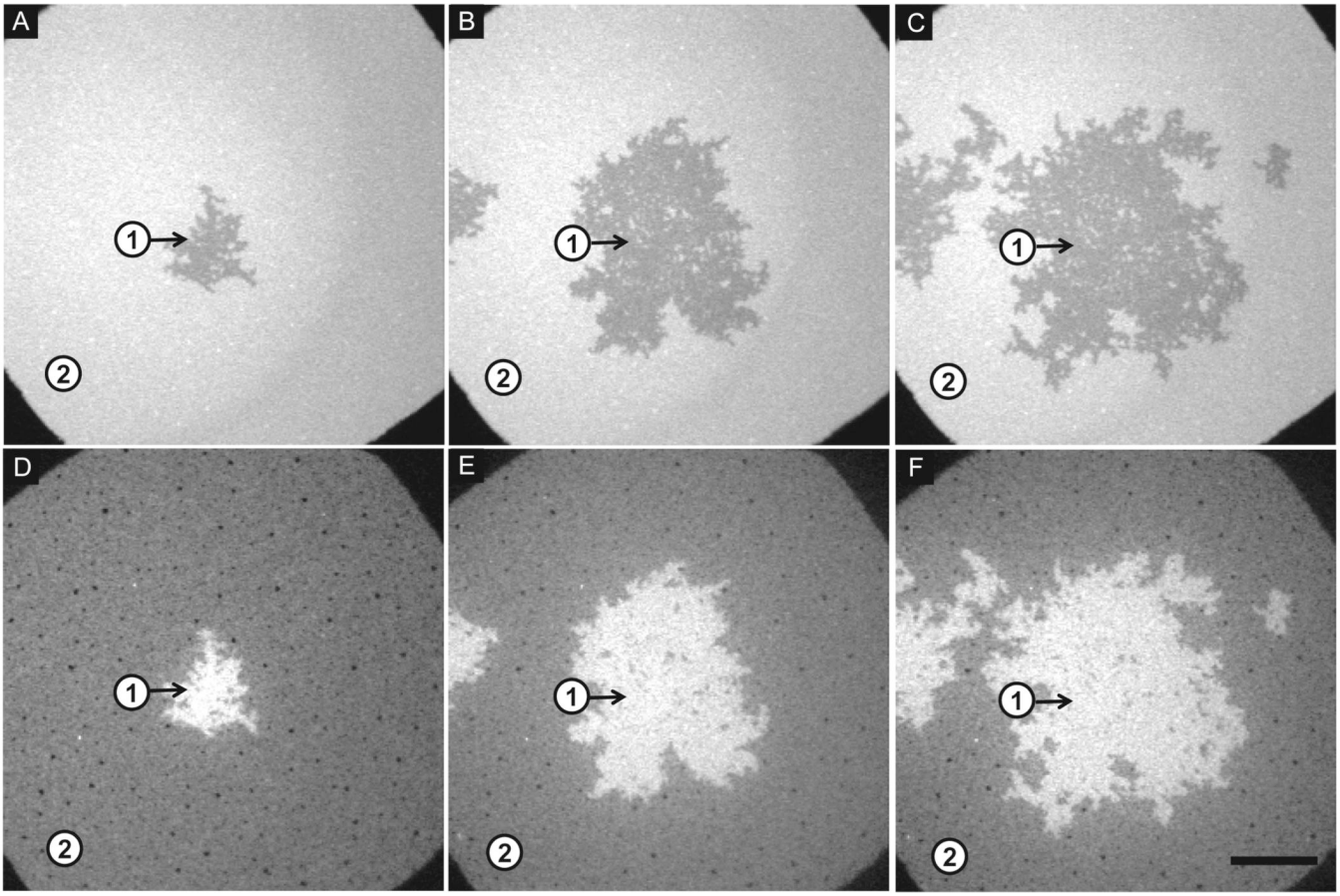

Figure 2.
Sequential addition of α-synuclein to a PA/PC bilayer at pH 7.4: Epi-fluorescence images of a 30 mol% DOPA/69 mol% DOPC/1 mol% NBD-PC bilayer at pH 7.4, 100 mM NaCl. Lipid bilayers (A–C) and corresponding protein images (D–F) are shown after successive additions of α-synuclein at 0.26 μM (A,D), 1.04 μM (not shown), 1.3 μM (B,E), 1.3 μM (not shown), and 1.3 μM (C,F). Two regions are highlighted: Region 1 (PA-rich); Region 2 (PC-rich). The scale bar represents 40 μm.

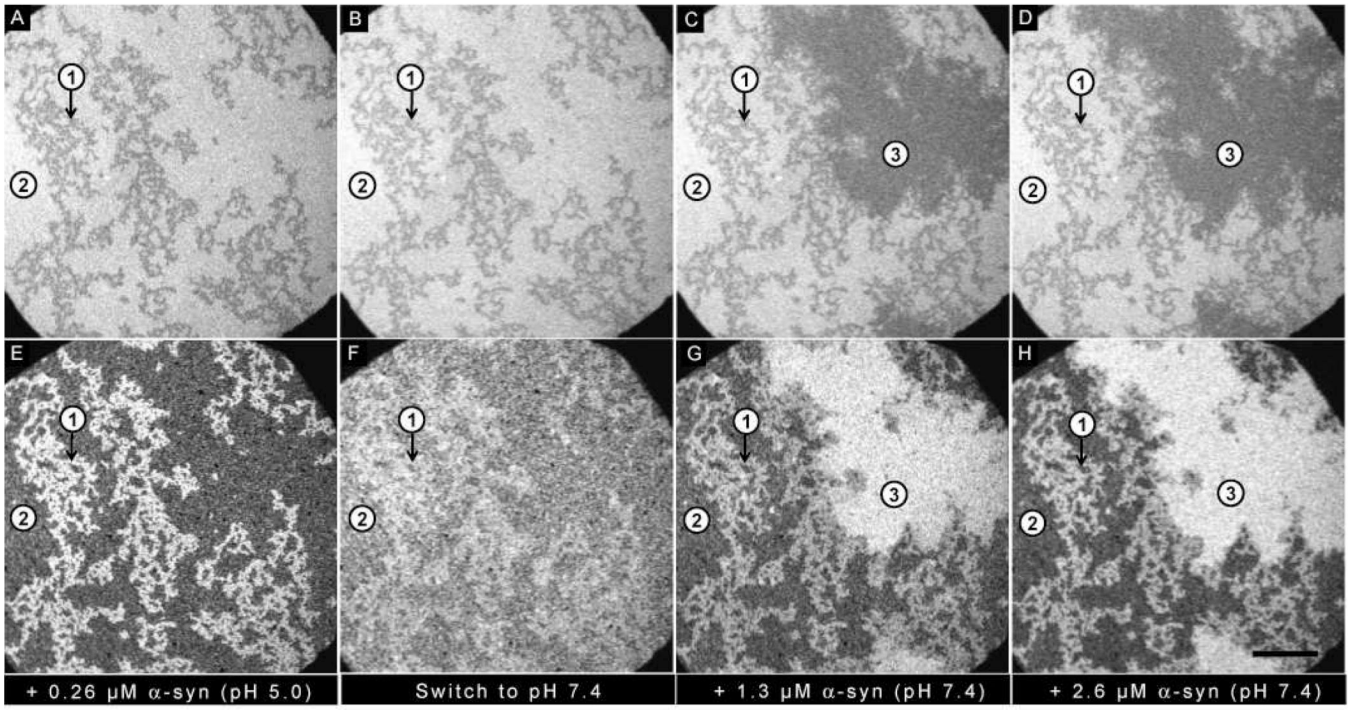

Figure 3.

Effect of switching the pH from 5.0 to 7.4: Epi-fluorescence images of (A–D) PA/PC bilayer and (E–H) α-synuclein. (A, E) Addition of 0.26 μM α-synuclein at pH 5.0. (B, F) Bulk pH was increased to 7.4. (C, D, G, H) Successive additions of 1.3 μM and 2.6 μM α-synuclein at pH 7.4. Three regions are highlighted: Region 1 (PA-rich); Region 2 (PC-rich); Region 3 (new PA-rich). The ionic strength of the solution was held constant at 100 mM. The scale bar represents 40 μm.

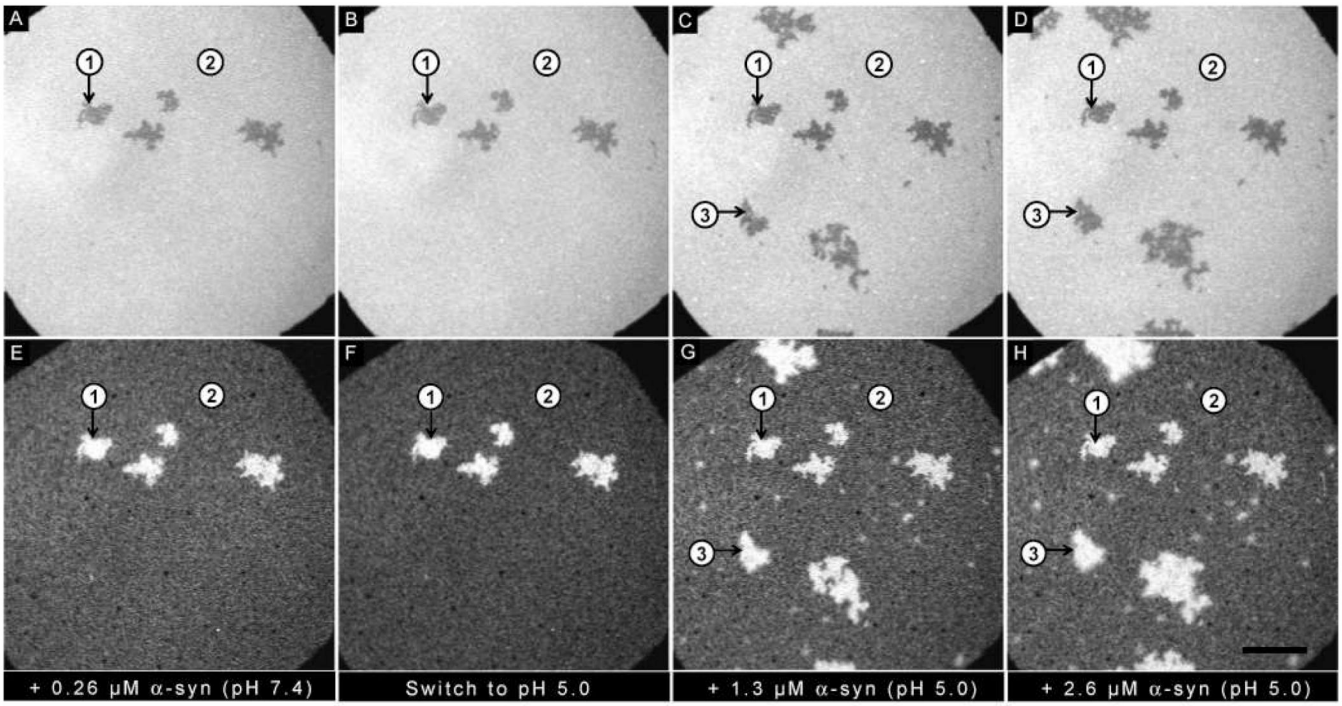

Figure 4.

Effect of switching the pH from 7.4 to 5.0: Epi-fluorescence images of (A–D) PA/PC bilayer and (E–H) α-synuclein. (A, E) Addition of 0.26 μM α-synuclein at pH 7.4. (B, F) Bulk pH was reduced to 5.0. (C, D, G, H) Successive additions of 1.3 μM and 2.6 μM α-synuclein at pH 5.0. Three regions are highlighted: Region 1 (PA-rich); Region 2 (PC-rich); Region 3 (new PA-rich). The ionic strength of the solution was held constant at 100 mM. The scale bar represents 40 μm.

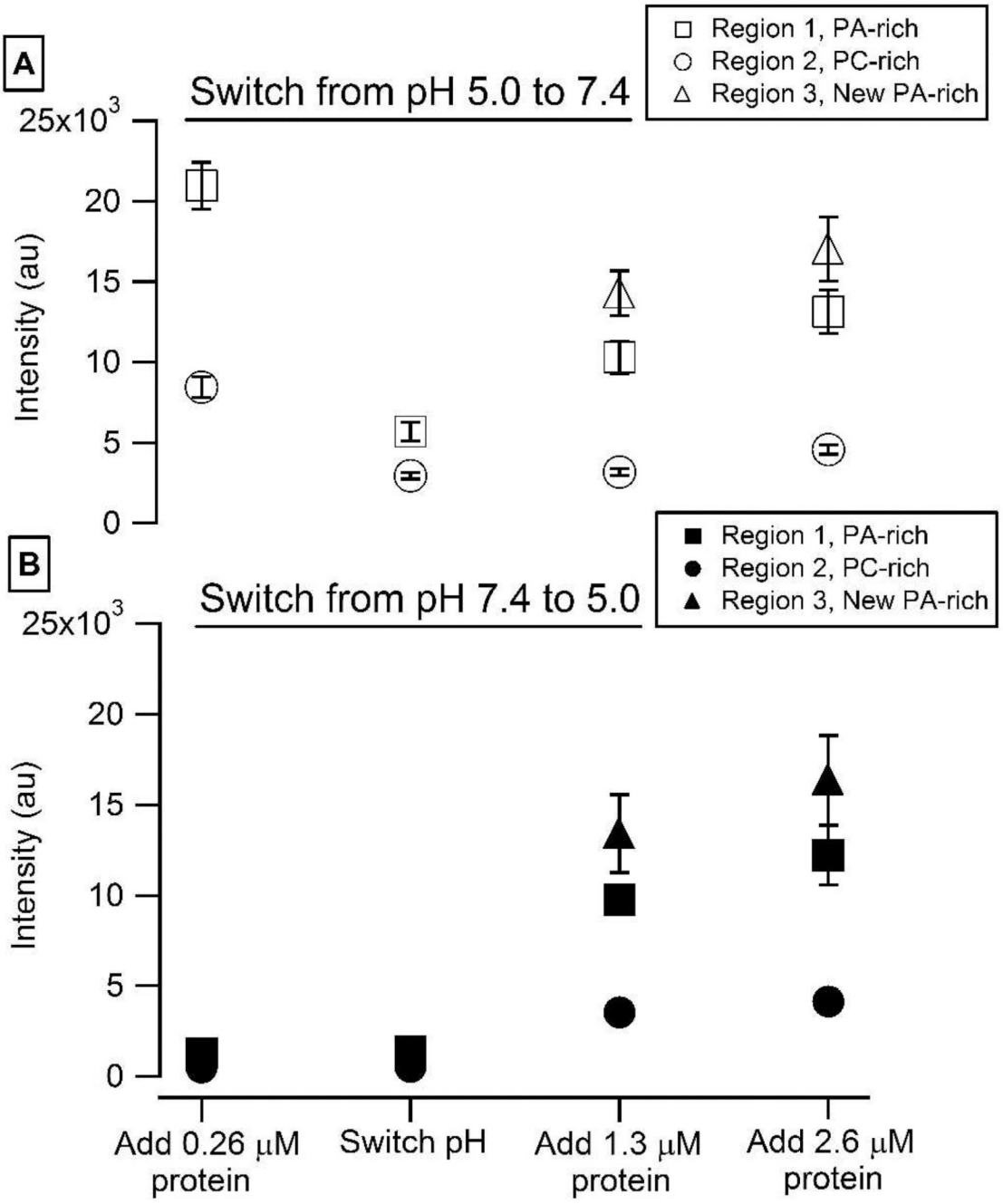

Figure 5.
Quantification of the amount of protein bound at each step in (A) Figure 4 and (B) Figure 5: Each data point represents the average of 12 samples. The error bars represent the standard deviation of the mean.

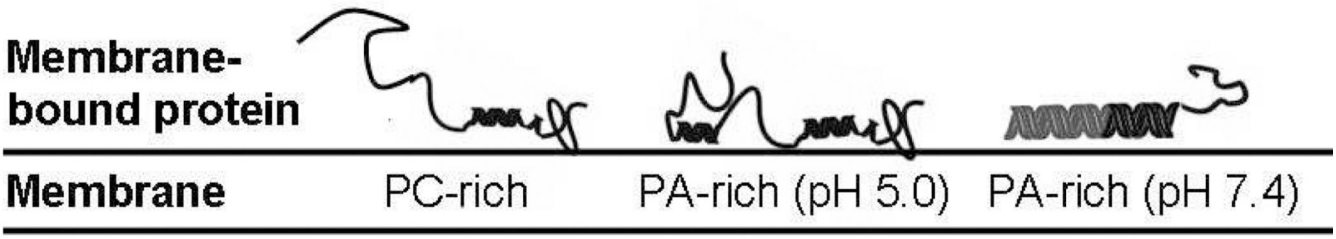

Figure 6.
Schematic illustration of the three possible adsorption sites created in Figure 3 and Figure 4. The helical content of the membrane-bound protein increases as the charge density of the underlying membrane increases.

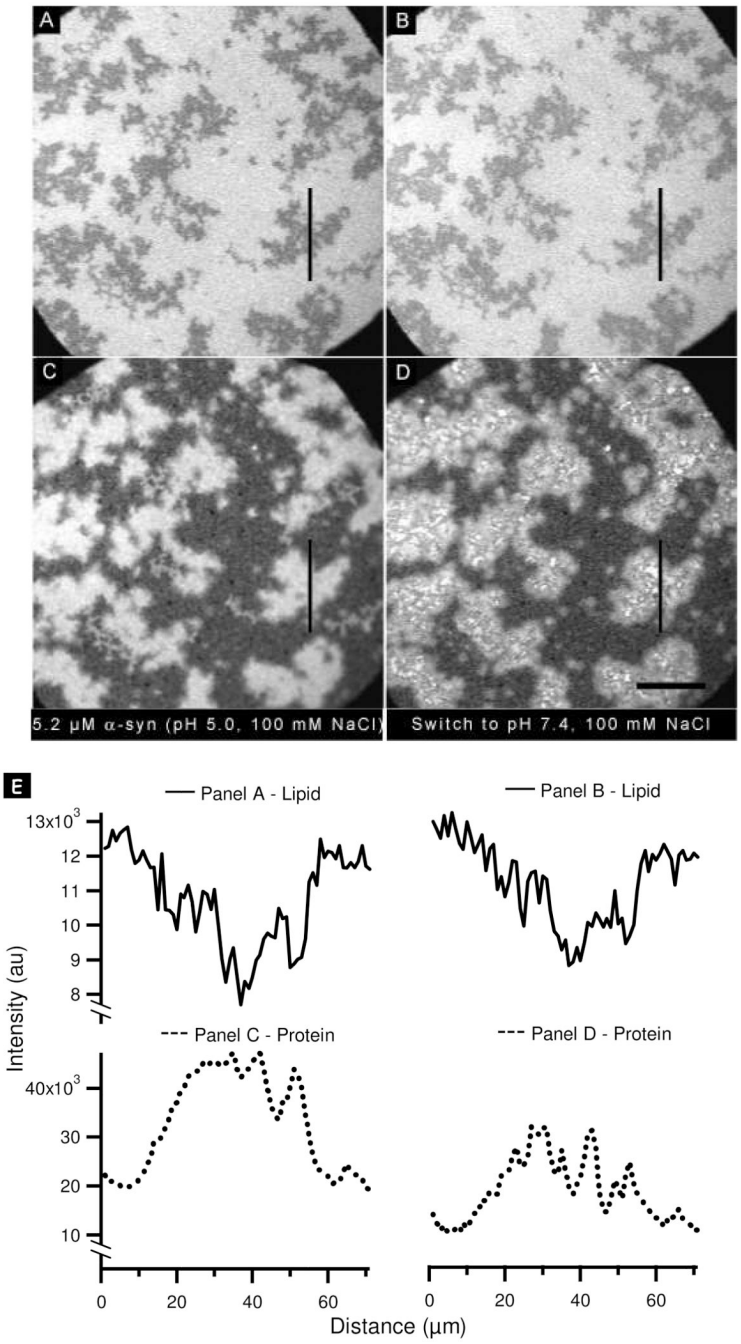

Figure 7.

Effect of switching the pH from 5.0 to 7.4 after the addition of 5.2 μM α-synuclein: Epi-fluorescence images of (A, B) PA/PC bilayer and (C, D) α-synuclein. (A, C) Addition of 5.2 μM α-synuclein at pH 5.0. (B, D) Bulk pH was increased to 7.4. (E) Lipid line scans (solid lines) and protein line scans (dotted lines) taken at the vertical lines in the images shown in panels A–D. The scale bar represents 40 μm.

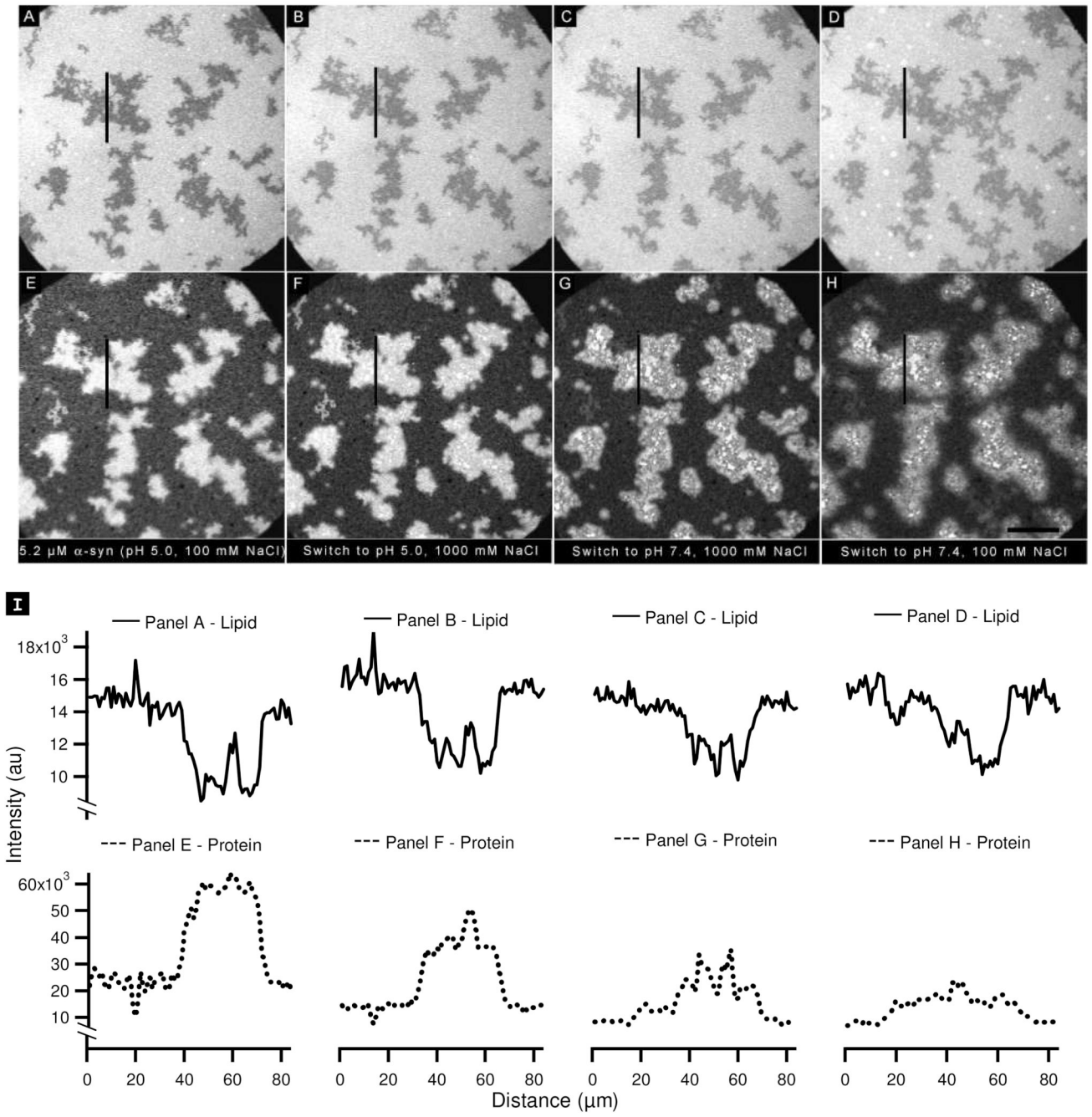

Figure 8.

Probing the stability of α-synuclein aggregates formed at pH 5.0 by changing the pH and ionic strength: (A, E) PA/PC lipid bilayer (A) and corresponding protein image (E) after the addition of 5.2 (μM α-synuclein at pH 5.0, 100 mM NaCl. (B–D, F–H) Lipid bilayers (B–D) and corresponding protein images (F–H) after successive changes to the bulk solution as follows: (B, F) the pH was kept constant and the NaCl concentration was increased to 1000 mM; (C, G) the NaCl concentration was kept constant and the pH was raised to 7.4; (D, H) the pH was held constant and the NaCl concentration was lowered to 100 mM. (I) Lipid line scans (solid lines) and protein line scans (dotted lines) taken at the vertical lines in the images shown in panels A–H. The scale bar represents 40 μm.

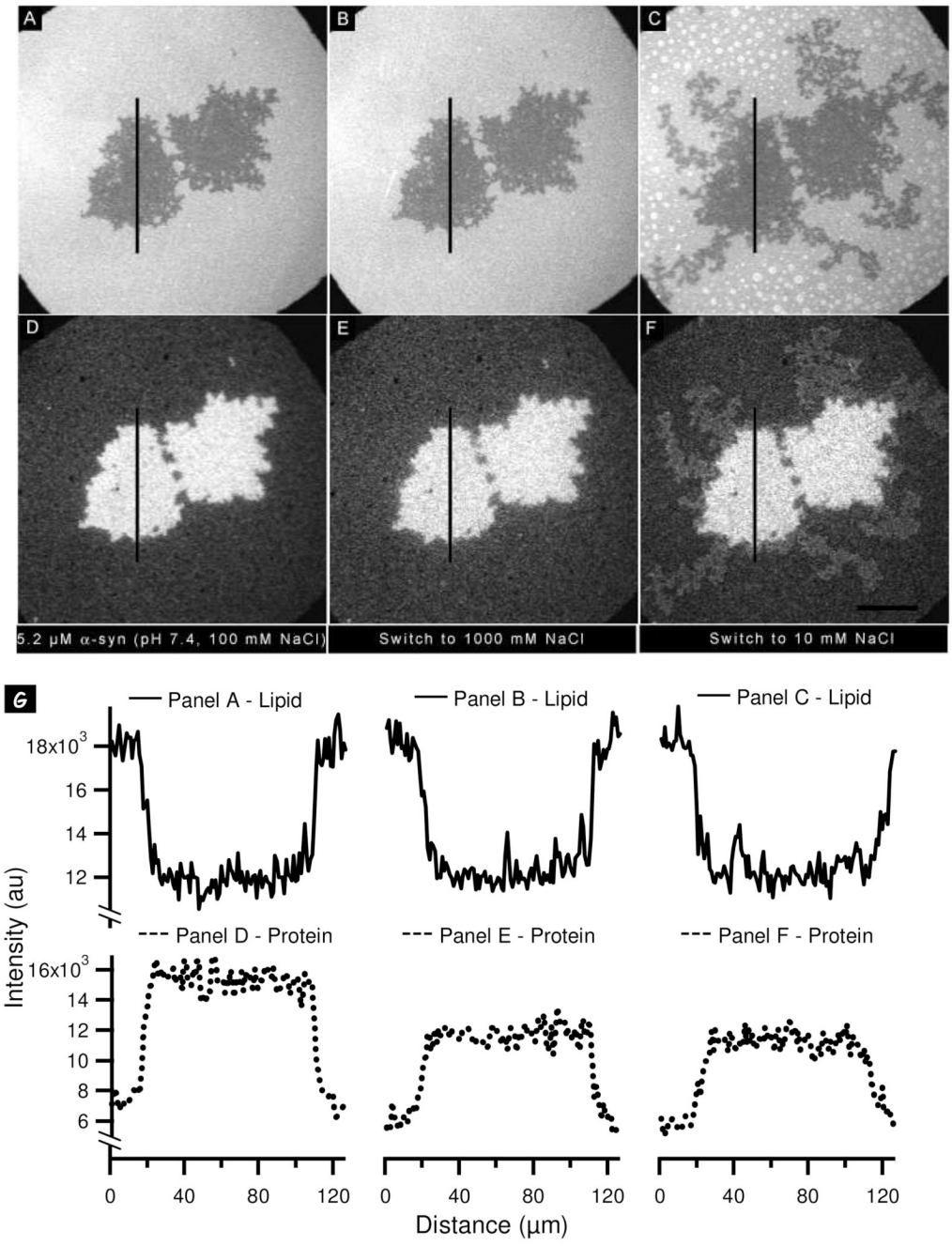

Figure 9.

Probing the stability of α-synuclein aggregates formed at pH 7.4 by changing the ionic strength: (A, D) PA/PC lipid bilayer (A) and corresponding protein image (D) after the addition of 5.2 (μM α-synuclein at pH 7.4, 100 mM NaCl. (B, C, E, F) Lipid bilayers (B, C) and corresponding protein images (E, F) after successive changes to the bulk solution as follows: (B, E) the NaCl concentration was increased to 1000 mM; (C, F) the NaCl concentration was lowered to 10 mM. (G) Lipid line scans (solid lines) and protein line scans (dotted lines) taken at the vertical lines in the images shown in panels A–F. The scale bar represents 40 μm.

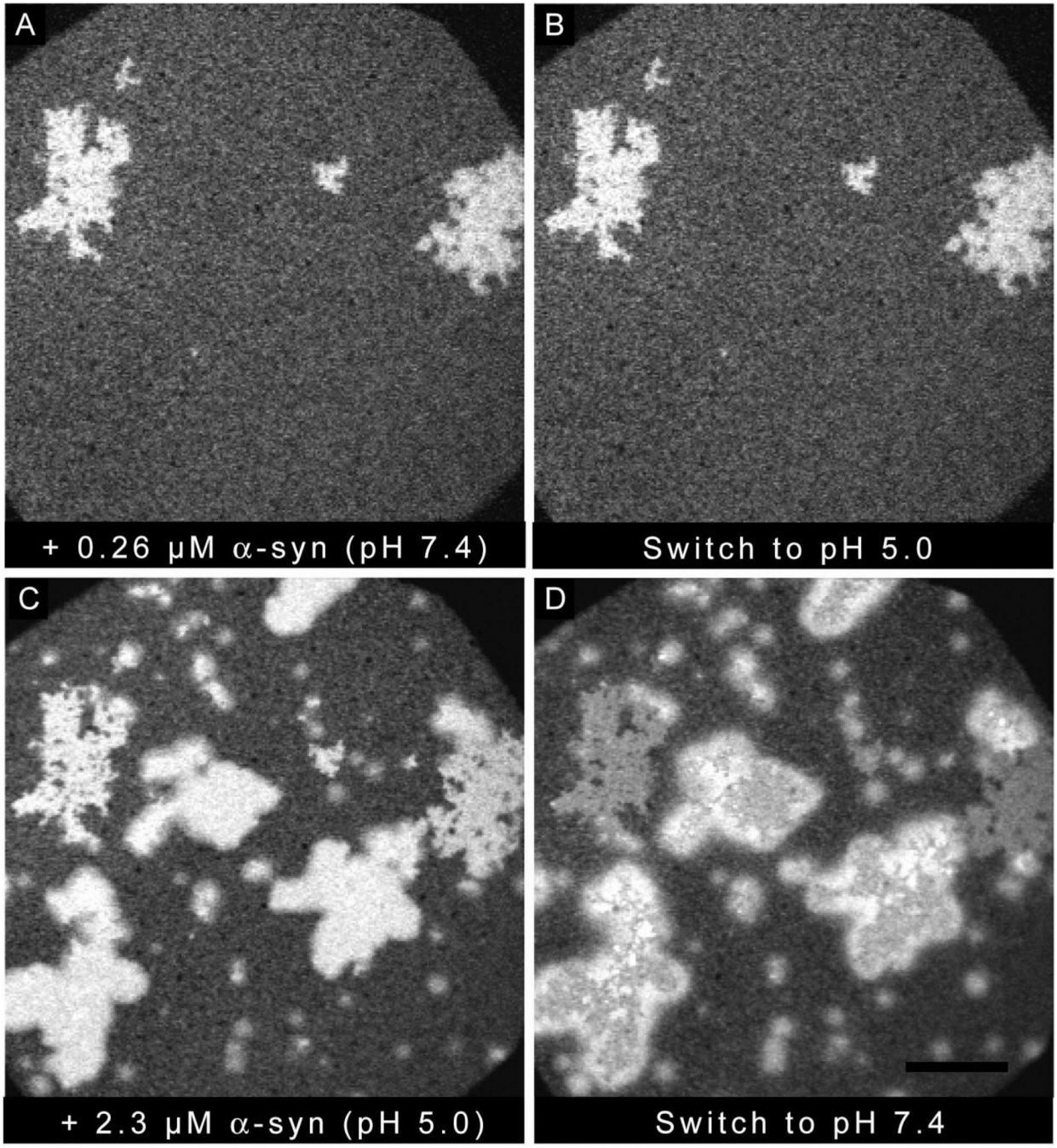

Figure 10.

Creation of structurally homogeneous and heterogeneous aggregates on the same bilayer: Protein images are shown after successively manipulating the solution conditions as follows: (A) 0.26 μM α-synuclein was added at pH 7.4, 100 mM NaCl; (B) the bulk pH was lowered to 5.0; (C) 2.3 μM α-synuclein was added at pH 5.0, 100 mM NaCl; (D) the bulk pH was increased to 7.4. The scale bar represents 40 μM.